

Experimental Evidence for New Pinning Conditions in Strongly Pinned Permalloy Film

Kyung Hunn Han^{1*}, Jae Hun Cho², and Sukmock Lee²

¹Plasma Laboratory, J&L Tech, Siheung 429-450, Korea

²Department of Physics, Inha University, Incheon 402-751, Korea

(Received 16 November 2006)

Experimental evidence suggests that spin pinning conditions for standing spin mode in polycrystalline Ni₈₄Fe₁₆ alloy film, is confirmed using the four categories of Camley *et al.* and the value of q_{\perp} for the pinning conditions, this was achieved by performing Brillouin light scattering measurements. The value of q_{\perp} was observed, in order to increase at a rate of $\pi/2$ with an increasing mode number. With this condition, the coexistence of standing spin wave modes was shown, with intermediate pinning, in addition to free and strong pinning. The values for spin-wave-stiffness constant (D_B), g -factor (g), and surface magnetization ($4\pi M$) of the Permalloy film were obtained from the results of BLS, and determined to be $D_B=1.85 \pm 0.05$ Oe cm^2 , $g=2.11 \pm 0.02$, and $4\pi M=8.7$ kG, respectively.

Keywords : Brillouin light scattering, permalloy film, surface anisotropy

1. Introduction

The Standing Spin-Wave (SSW) modes were first observed in thick Permalloy film by Spin-Wave Resonance (SWR) in 1958 [1]. Kittel predicted that the possibility of exciting these spin-wave modes exists, when spins were pinned at a minimum of one boundary of the film [2]. Searle *et al.* observed in the Permalloy film that the positions of mode shifted from one position to another, within the limited two boundary surfaces. This demonstrated that the observed shift in positions of mode could be described by introducing a phase shift to the perpendicular component of the wave vector [3]. The phase shift is a direct measure of the degree of pinning, the pinning mechanisms have been proposed as an effect of Néel surface anisotropy or the existence of interaction with an antiferromagnetic surface layer [2, 4]. Since then, much work has been made to relate to the behavior of SSW modes excited by the pinned spin studied by SWR [5, 6].

It is crucial for the dynamics of the soft magnetic materials to be understood, as dynamics for spin pinning are governed by internal demagnetizing fields during the switching processes. In addition, the understanding of its

spin pinning phenomena is of interest, not only from basic physics but also from a technological point of view. With this information, it is possible to understand the response and precessional frequency of the spin. This is very important for switching applications such as the engineering high-performance recording systems.

Brillouin light scattering (BLS) has been used to study thermally excited SSW and surface wave modes in magnetic materials [7-9]. The BLS spectrum provides the frequencies of spin wave for the range of wave vector q values 10^3 - 10^6 cm⁻¹. One of many properties studied by BLS included the presence of spin pinning on the SSW modes. With regard to spin pinning, when the Zeeman field is parallel to the film surfaces, the spins on one surface experience an effective pinning field antiparallel/perpendicular to the applied Zeeman field. The Stokes and anti-Stokes lines for the SSW modes were known to show the asymmetric intensities in such a pinning condition. Malozemoff *et al.* have discussed the presence of pinning using a simple formula between the exchange field and optical properties [8]. Camley *et al.* have discussed the four pinning conditions with numerical analysis, including spin pinning at both the upper and the lower surfaces [10]. It is possible to determine the characteristics of pinning by observing the intensity of the SSW modes in both Stokes and anti-Stokes scattering. However,

*Corresponding author: Tel: +82-31-499-1005,
Fax: +82-31-499-1006, han.kyunghunn@gmail.com

despite efforts to explain the behavior of abnormal SSW modes in the BLS field, a phase shift in the positions of the mode has not yet been experimentally observed. Several authors have observed the BLS spectra for the critical angle behavior and in-plane wave number dependence of surface wave mode in the case of thin Permalloy films [11, 12].

In this study the characteristics of the pinning is investigated with these two models, and a different behavior of SSW modes is described, such as a phase shift, on the Permalloy film with surface pinning.

The $\text{Ni}_{84}\text{Fe}_{16}$ films were prepared by means of a dc magnetron sputtering system, using a commercial $\text{Ni}_{80}\text{Fe}_{20}$ target on the Si(100) wafer. The thickness of the film was prepared as $d = 109 \pm 1.6$ nm. The magnetic and structural properties of the prepared films were examined using a Vibrating Sample Magnetometer (VSM) and X-Ray Diffraction (XRD) at room temperature. The XRD results indicate that the prepared films consist of polycrystalline with an almost three-dimensional random orientation, and without any other crystal phase. The magnetization (M_s) and coercivity (H_c) values were found to be 687.1 ± 10 emu/cm³ ($4\pi M_s \sim 8.6 \pm 0.1$ kG) and ~ 2 Oe, respectively. The spin waves are studied by a Sandercock-type (3+3) multipass tandem Fabry-Perot interferometer [13]. The excitation light source is a single longitudinal mode of the 514.5 nm line of an argon ion laser, with an output power of 250 mW. The accumulation time for each spectrum was approximately 20 min.

Fig. 1 presents a representative spin-wave Brillouin Spectrum (BS) for the sample with a thickness of 109 nm in the presence of an external magnetic field $H_0 = 1.2$ kOe. The stronger peak observed on the anti-Stokes region had its origin in scattering from the surface wave, localizing on the laser illuminated surface. For ferromagnetic thin film, the surface wave is known as the Damon-Eshbach mode (DE mode). A series of the SSWs is also observed. Fig. 2 presents the deconvolution of the spin-wave spectra in Fig. 1, by showing several Lorentzians with line-width of about 3.8 GHz. As presented in Fig. 2, the relative intensity of SSW lines shows monotonically decreasing intensity with a frequency on the Stokes side, whereas on the anti-Stokes side, the intensities tend to increase. This anomalous behavior of the intensities of the SSWs can be explained as an indication of a pinning condition. In order to determine the magnetic constants, the spin-wave frequencies are measured as a function of the magnetic field, displayed in Fig. 3. The in-plane wave vector of the spin waves with an external field set at 0.6 kOe, are presented in Fig. 4. The dependence of DE mode and the first SSW, both on the magnetic field and on the in-plane wave

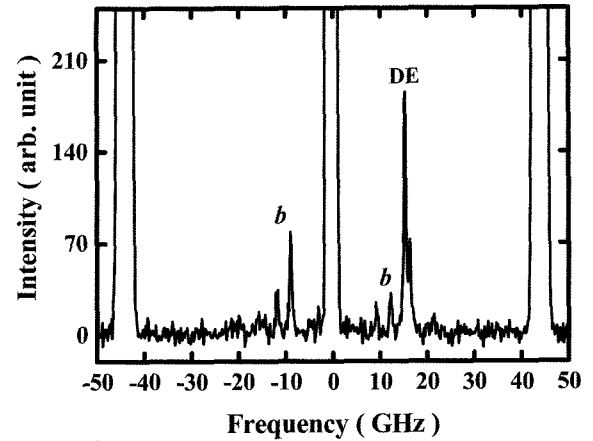


Fig. 1. SW Brillouin spectra observed from the sample at incident angle θ_i of 45° in $H_0 = 1.2$ kOe. The large peak labeled "DE" represents the Damon-Eshbach mode, the smaller peaks labeled by "b" which occur at both positive and negative frequency are produced by scattering from SSW modes of the film.

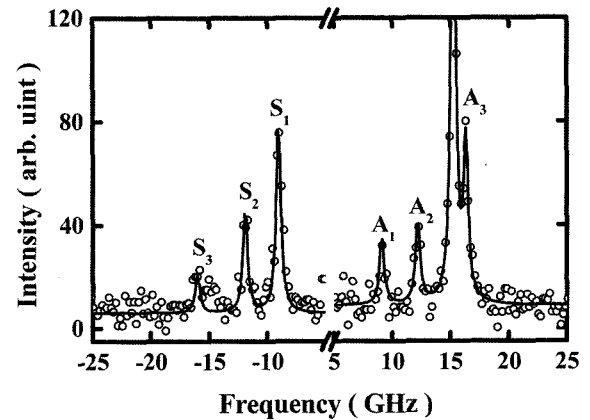


Fig. 2. Intensity of the Stokes and anti-Stokes spin-wave spectra in the sample to the DE and SSW modes at $\theta_i = 45^\circ$ and $H_0 = 1.2$ kOe, respectively. The DE mode is labeled by DE and S_n and A_n ($n = 1, 2, 3, \dots$) denote the Stokes (S) and anti-Stokes (A) SSWs, respectively. Here, the n refers to the mode number of the SSWs. The omitted frequency region ($-5 \sim 5$ GHz) is an artifact of the interferometer used to remove the elastic Rayleigh peak. The intensity of each peak obtained using the Lorentzian function is demonstrated by the solid line. The open circles are the experimental points.

vector, have been used to fit to a spin-wave theory according to the procedure in the references [7-11] with a condition of $\exp(-q_{\parallel}d) \ll 1$. A set of magnetic parameters was found: $g = 2.11 \pm 0.02$, $4\pi M = 8.7$ kG, $D_B = 1.85 \pm 0.05$ Oe \cdot cm², and $A = 0.64 \pm 0.01 \times 10^{-6}$ erg/cm. Here, D_B and A are the spin-wave stiffness constant and the exchange constant, respectively. The internal effective field H_a was introduced as an effective magnetic field. The effective magnetization resulting from the competition

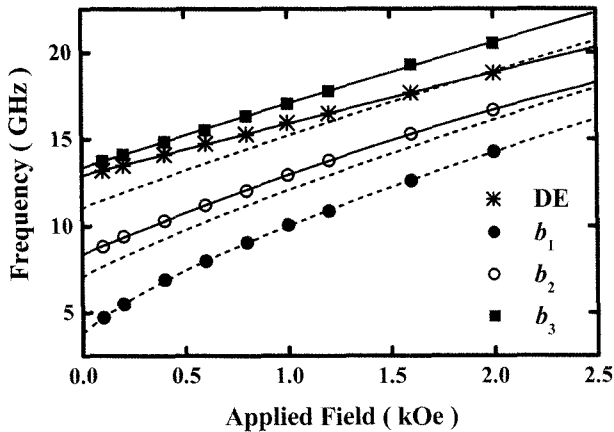


Fig. 3. External magnetic field dependence of DE and SSW modes frequencies obtained the sample with $q_{\parallel} = 1.72 \times 10^5 \text{ cm}^{-1}$. The b_n 's are the absolute values of the measured frequency for both Stokes and anti-Stokes SSW peaks. The solid and broken curves result from least-squares fits of magneto-static spin-wave theory with the magnetic constants.

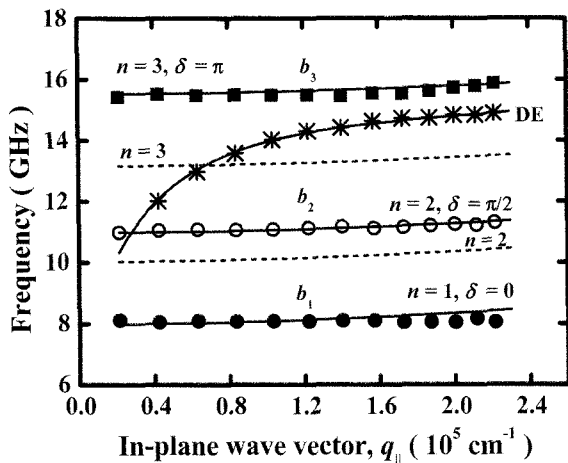


Fig. 4. The variation of frequency with change of in-plane magnon wave number in a constant magnetic field of 0.6 kOe for the sample. The same symbols in Fig. 3 are used for each spin-wave mode. The solid and broken lines demonstrate the fit obtained using magnetostatic spin-wave theory with the magnetic constant obtained from Fig. 3.

between $4\pi M$ and H_a can be given by $4\pi M_{\text{eff}} = 4\pi M - H_a$, where $H_a = 2K_s/M$ with K_s being the surface anisotropy constant. This method is the same simplified approach used in Ref. 14. The internal effective field is determined to be $H_a = 70.9 \text{ Oe}$, with the magnetic constants determined as above, from the surface spin-wave frequency as a function of the in-plane wave vectors. $K_s = 0.284 \pm 0.013 \text{ erg/cm}^2$ is then obtained from the result of H_a for the sample, and the K_s is comparable to the value reported by Maksymowicz *et al.* [6] for the Ni_3Fe film with thickness of 90 nm deposited by electron beam evaporation ($K_s =$

0.29 erg/cm^2). The theoretical lines, calculated with the best-fit parameters, are plotted in solid (DE and SSWs) lines in Fig. 3 and 4. The magnetization ($4\pi M$) for the sample, determined by the BLS measurement, is congruent with the value obtained from the VSM measurement. The other parameters determined in this study are also congruent with those in the references [6 and 7].

In Figs. 3 and 4, the second and third SSWs present a certain difference between the experiments and theories. This discrepancy was combined with the anomalous behavior in intensities, in order to demonstrate the additional pinning condition with appropriate phase shifts in the SSW modes. In order to apply the pinning conditions that Camley *et al.* [10] used for the standing waves propagating perpendicular to the direction of magnetic moment, to the intensities of the SSWs, the intensity ratios A_2/A_1 (denoted as "A₁₂" hereafter) and S_2/S_1 (denoted as "S₁₂" hereafter) are determined, where S_1 , S_2 , A_1 , and A_2 are the intensities of the first and the second SSWs in the Stokes and anti-Stokes components of the spectrum, respectively. The ratios S_{12} and A_{12} are approximately 1.7 and 0.9, respectively, in the experimental results, this combination does not belong to the four categories of spin pinning, suggested by Camley *et al.* However, if the four categories of surface pinning are separated into components in terms of A_{12} and S_{12} , it can be found that A_{12} and S_{12} indicate the bottom and top surfaces, respectively, these magnitudes express the degree of pinning near each surface. From this combination it can be indirectly suggested that the bottom surface is subjected to the strong pinning field but the top surface is free. From the point of view of this problem, the sample used in this work can also be speculated and included in some other pinned conditions, besides the pinned condition on top and/or bottom surfaces. As well-defined evidence used to support such presumptions, the pinning configuration is investigated in the perpendicular component of the wave vector. As presented in Figs. 3 and 4, the second and third SSWs are in disagreement with first SSW, satisfying the condition of $q_{\perp} = n\pi/d$. This result indicates a possible phase shift that could be caused by inhomogeneities in the standing wave. The perpendicular component of the wave vector given by $q_{\perp} = (n\pi + \delta_n)/d$ with $n = 0, 1, 2, 3, \dots$ [10] can be used. Here, δ_n is a phase shift lying between 0 and π , and depending on the pinning condition at the boundary. The value of δ_n obtained for the sample, tends to increase with n as $\delta_n = 0$ ($n = 1$), $\pi/2$ ($n = 2$), and π ($n = 3$). SSWs dispersion is plotted by solid and broken lines in Fig. 3 and 4. The results for this experiment are explained as follows. The $n = 1$ mode is the unpinning state with a node at the center and the antinodes at both ends. The $n =$

3 mode is the pinning state, transforming to the $n = 4$ mode, while in the case of the $n = 2$ mode, the mode shape may be excited by a spin-wave mode with a node at one side (start) and the antinode at other side (end), within the boundary. The $n = 2$ mode then indicates an intermediate pinning state. Finally, it is noted that the observed pinning state of the sample is most likely one of three cases, free, intermediate, and strong pinning. It is seen that apparently higher order modes are pinned stronger than the low order modes, this claim is well supported in this paper.

In addition, an analysis discussion by Malozemoff *et al.* [8] was also applied for the exchange field H_{ex} ($=D_B q^2$). The peak of the SSW modes is noted for shifting from $H_{ex} = 0$ to pinning field H_p ($=D_B \alpha^2/4$) in the presence of strong pinning. Here, α is the absorption coefficient, defined by $\alpha = 4\pi\kappa/\lambda$. κ is the extinction index of the refraction index. When the discussions by Malozemoff *et al.* are followed, the relationship between H_{ex} and H_p can be calculated using the optical constant ($\kappa = 3.2$) for the 90 at.% of Ni at $\lambda = 500$ nm [15]. $H_p = 282.5$ Oe is obtained from the result of D_B and $\alpha = 7.82 \times 10^5$ cm⁻¹ for the sample with the wavelength ($\lambda = 514.5$ nm). H_{ex} is also determined to be 208.9 Oe with the D_B , $q_{||} = 1.727 \times 10^5$ cm⁻¹, and $q_{\perp} = n\pi/d$ with $n = 1$ obtained from experimental measurements. It is found that the value of H_p is greater than that of H_{ex} . The H_a ($= 70.9$ Oe) obtained by effective magnetization is found to be similar to the difference ($= 73.7$ Oe) between H_p and H_{ex} . From the above numerical consideration, it is found that the amount of pinning is explained by the correction of the exchange field coupled by light rather than the asymmetry of intensity caused by the pinning.

In summary, the various behaviors of pinning can be examined by DE and SSW modes in Ni-rich Ni-Fe alloy thin film, with a thickness of approximately 109 ± 2 nm by BLS at room temperature. The degree of pinning was investigated using the ratio of intensity on the SSWs at

both Stokes and anti-Stokes regions and effective exchange correction of order. The configuration of pinning was also observed by the boundary condition, with wave vectors perpendicular to the surface. It indicated that pinning does not occur at the top surface, whereas strong pinning is dominant at the bottom surface. In addition to the four categories displayed, an existence of another pinning condition is demonstrated.

References

- [1] M. H. Seavy, Jr., and P. E. Tannenwald, *Phys. Rev. Lett.* **1**, 168 (1958).
- [2] C. Kittel, *Phys. Rev.* **110**, 1295 (1958).
- [3] C. W. Searle, A. H. Morrish, and R. J. Prosen, *Physica*, **29**, 1219 (1963).
- [4] P. Pincus, *Phys. Rev.* **118**, 658 (1960).
- [5] G. C. Bailey and C. Yittoria, *J. Appl. Phys.* **8**, 3274 (1973).
- [6] A. Z. Maksymowicz, J. S. S. Whiting, M. I. Watson, and A. Chambers, *Thin Solid Films*, **197**, 287 (1991).
- [7] P. Grünberg, C. M. Mayr, and W. Vach, *J. Magn. Magn. Mat.* **28**, 319 (1982).
- [8] A. P. Malozemoff, M. Grimsditch, J. Abosf, and A. Brunsch, *J. Appl. Phys.* **50**, 5885 (1979).
- [9] A. Yoshihara, Y. Haneda, Y. Shimada, and T. Fujimura, *J. Appl. Phys.* **66**, 328 (1989).
- [10] R. E. Camley, T. S. Rahman, and D. L. Mills, *Phys. Rev. B* **23**, 1226 (1981).
- [11] G. Srinivassan and C. E. Patton, *J. Appl. Phys.* **61**, 4120 (1987).
- [12] H. Moosmuller, J. R. Truedson, and C. E. Patton, *J. Appl. Phys.* **69**, 5721 (1991).
- [13] R. Mock, B. Hillebrands, and J. R. Sandercock, *J. Phys. E: Sci. Instr.* **20**, 656 (1987).
- [14] S. Tacchi, L. Albini, G. Gubbiotti, M. Madami, and G. Carlotti, *Surf. Sci.* **507-510**, 535 (2002).
- [15] N. B. De Cristofaro, D. Huerta, and K. E. Heusler, *Electrochimica Acta* **35**, 69 (1990).